Random packings of spheres and spherocylinders simulated by mechanical contraction

S. R. Williams and A. P. Philipse
Van 't Hoff Laboratory for Physical and Colloid Chemistry, Debye Institute, University of Utrecht, Padualaan 8, 3508 TB Utrecht, The Netherlands

(Received 21 October 2002; published 7 May 2003)

We introduce a simulation technique for creating dense random packings of hard particles. The technique is particularly suited to handle particles of different shapes. Dense amorphous packings of spheres have been formed, which are consistent with the existing work on random sphere packings. Packings of spherocylinders have also been simulated out to the large aspect ratio of $\alpha=160.0$. Our method packs randomly oriented spherocylinders to densities that reproduce experimental results on anisotropic powders and colloids very well. Interestingly, the highest packing density of $\phi=0.70$ is achieved for very short spherocylinders rather than spheres. This suggests that slightly changing the shapes of the particles forming a hard sphere glass could cause it to melt. Comparisons between the equilibrium phase diagram for hard spherocylinders and the densest possible amorphous packings have interesting implications on the crystallization of spherocylinders as a function of aspect ratio.

DOI: 10.1103/PhysRevE.67.051301 PACS number(s): 81.05.Rm

I. INTRODUCTION

In nature and technology, a wide variety of amorphous structures can be found, which consist of randomly packed nonspherical particles. Macroscopic examples are packings of rice, grass seed, gravel, and glass fibers in reinforced composite materials [1]. Also on the mesoscopic length scale, random packings are well known, such as for cellulose fibers in paper [2] and other fibrous media [3,4] and colloidal rods in amorphous sediments [5]. The density of such packings forms an intriguing, largely unsolved problem. The topic of random packing densities has a long and extensive history [6–8] which, however, almost exclusively deals with the limiting case of spheres. At first sight, this focus on spheres may seem reasonable; one expects that nonsphericity will always complicate the packing density problem due to the additional complexity in considering particle orientations. It has also been pointed out, however, that isotropic thin rods may actually form more simple random packings because correlations for thin rods are much weaker than for spheres [5]. Of course, it is desirable that an approach (or even an explanation) for random packing densities is found, which is sufficiently general to include the effect of particle shape. The aim of this work is to introduce such an approach in the form of a simulation technique that appears to be very suitable for creating amorphous packings of spheres as well as fibers up to very high aspect ratios. The method should be readily applicable to other shapes such as disks (amorphously packed in three dimensions) or ellipsoids and to packings in other dimensions.

One incentive for our work is the experimental observation that packing volume fractions of randomly oriented rigid fibers, in comparison to spheres, drastically decrease with increasing particle aspect ratios [1,5,9–14] in a manner that is invariant to the particle's size. This trend has been reported for rod lengths that span many orders of magnitude from colloidal rods in the nanometer size range [5] to chopped raw spaghetti [13] on the centimeter scale. This size invariance clearly shows that random packing densities have a purely geometric origin, an assessment that also forms the basis of our simulation method (see Sec. II C). Experiments also indicate that the packing volume fraction ϕ tends to zero for long rods as the aspect ratio increases according to the asymptotic scaling [5],

$$2\phi\alpha=\langle\gamma\rangle=2c \quad \text{for} \quad \alpha\gg 0. \tag{1}$$

Here, $\alpha=L/D$ is the aspect ratio for a rigid thin rod of length L and diameter D, $\langle\gamma\rangle$ is the average number of contacts experienced by a given particle, and according to the experiments the contacts per particle c is 5.4 ± 0.2. This scaling, first noted in Ref. [11] and discussed by several authors [2,5,9,10], can be explained by a simple excluded volume argument [5] as will be further discussed in Sec. III. However, alternatives to Eq. (1) have been proposed such as an exponential [15], logarithmic [13], and a nonanalytic [7] dependence of the random rod packing density on aspect ratio α. To confirm the correct scaling for thin rods, simulation results are needed at high aspect ratios (say $\alpha>50$), which are experimentally difficult to handle due to unwanted particle flexibility and possibly particle alignment. Unfortunately, the simulations we are aware of only deal with small aspect ratios [9,16] and, moreover, produce densities that are clearly below experimental values [5]. Thus, our first goal is to extend simulations to higher aspect ratios with a meaningful model of the experimental systems.

Our second goal is to investigate the opposite limit, namely, what happens if the particle shape approaches that of a sphere. The issue here is whether the Bernal random sphere packing (with a volume fraction $\phi\simeq0.64$) is a maximum in the packing density as a function of aspect ratio. Earlier work of Sherwood [16] and others [17–19] suggest that spheres may form a local minimum. However, the results [16,19] were difficult to interpret as the limiting density for spheres was substantially below the Bernal packing density of $\phi=0.64$. Clearly, this limit should at least be correct; further a

plausible geometric explanation for any increase in volume fraction, due to a small deviation from the spherical shape, needs to be formed.

Our third goal, once having random packing densities from spheres up to very thin rods, is to make a comparison to thermodynamic systems. The Bernal sphere packing has a density that is higher than the hard sphere crystal's melting point of $\phi=0.545$ [20], above which the equilibrium state becomes a single-crystal phase. It would be interesting to know what happens at finite aspect ratios of spherocylinders. Are random packings always at a higher density relative to an equilibrium crystalline phase with either positional or orientational ordering? Such information is important to better understand the often puzzling phase behavior of colloidal rods quenched into random packings by rapid sedimentation [21].

The content of this paper is as follows. Sections II A and II B briefly review existing methods to simulate random (or granular) packings and motivate the need for a mechanical contraction technique, which is explained in Sec. II C. The resulting random packing densities are discussed in Sec. III, a comparison is made to the random contact equation in Sec. III C and to existing experimental data and equilibrium phase behavior in Sec. III D. Implications on the glass transition are discussed in Sec. III E.

II. METHODS FOR SIMULATING GRANULAR PACKING

A. Existing work

Simulation methods for forming granular packings of hard particles can be placed in two distinct groups. The first group, referred to as concurrent algorithms, involves the densification of a fixed number of particles. The second group, referred to as sequential algorithms, involves progressively adding more particles to a fixed volume.

Concurrent algorithms have been used to obtain granular packings of disks in two dimensions and spheres in three dimensions. Random packings of disks are unstable to vibrations, which cause them to crystallize [22]. However, an amorphous packing with an area coverages of $\phi=0.77$ has been achieved using an algorithm that avoids local crystalline regions [23]. Random packings of spheres have been obtained with a variety of volume fractions $0.60<\phi<0.68$ [24]. Volume fractions above $\phi=0.64$ require more order in the system [24], typically induced by further vibrational exploration during the quench when the quench rate is not rapid enough or the quenching mechanism (of the particular algorithm) is not aggressive enough. A detailed simulation technique has recently been reported, here the effects of friction, particle softness, and energy dissipation have been studied on the granular packing of spheres [25]. Under conditions of finite pressure (due to gravity), it was found that frictional forces, in particular, could affect the final volume fraction and coordination number of the system.

Studies employing sequential algorithms have been reported for disks [26], spheres [27], ellipsoids [16], and spherocylinders [9]. All these studies have employed a technique known as random sequential addition (RSA). The area coverage for disks was found to be $\phi=0.547$, while for three-dimensional spheres a volume fraction of $\phi=0.385$ was found. The studies on ellipsoids and spherocylinders have been limited to aspect ratios α such that $0.067<\alpha<25$. While the obtained aspect ratio dependence is qualitatively similar to experimental results [5], the volume fractions are significantly less than experimental packings. In general, the RSA method obtains final packing densities, which are significantly lower than what is found from experiments and more realistic concurrent algorithms.

An important definition is that of a jammed state. Here we define this (solely for computer simulations) as the state where any extension of computational effort, using a given algorithm, fails to increase the systems density. Under this definition, concurrent algorithms often produce a jammed state while RSA does not. Obviously, this definition may depend upon the algorithm being employed.

B. Existing methods for simulating granular packing

Several methods have been employed to simulate granular packings. It should be pointed out, from the outset, that when it comes to the packing of rods or fibers, all these techniques have some very serious shortcomings. For this reason, we have developed a technique that will be discussed in Sec. II C. One of the earliest methods used to obtain dense amorphous packings of hard disks and spheres was based around molecular dynamics [28], using an equilibrium fluid as a starting point. Having used this method, we will discuss a shortcoming it has in forming granular packings. When two particles approach each other dominantly due to their own expansion rather than their thermal velocities, an elastic collision will result in a postcollision separation rate, between the two particles centers, which is less than the rate at which the particles are expanding. This results in the pair of particles expanding inside each other. Including some form of inelastic collision in the event of the above occurrence can alleviate this problem; however this will result in the system's temperature increasing and the effective quench rate decreasing. As a granular packing is approached, the collision rate will diverge and, in turn, so will the rate at which the temperature is increasing. Considering how sensitive the formation of local crystalline environments is on the quench rate in these systems, this is a serious problem when simulating random packings. Of course, all the particle velocities could be equally scaled down, to compensate for the extra energy introduced in the event of an inelastic collision, by which stage the method has lost all its initial simplicity. While this is a sound simulation method, it is already difficult enough with spheres, we decided to make no attempt to generalize it to include rods.

A novel method used by Hinrichsen, Feder, and Jøssang [23] was to form a Voronoi tessellation around a system of disks. The disks were then all moved to the center of their Voronoi cell and the system was squashed as much as possible (scaling the particle positions) until a pair of disks came into contact with each other. This was then repeated until the system could no longer be reduced in volume and thus a random packing was obtained. The motivation behind this method was to obtain a dense amorphous packing of disks

without any crystallization processes taking place. While this method could obviously be extended to spheres, it is not so obvious how to extend it to the case of rods.

Another method we have tried in our exploration of random rod packings is based around a Monte Carlo simulation. A standard Monte Carlo simulation is carried out to obtain an equilibrium fluid. At random intervals, the volume is reduced, with all the particle positions being scaled until a pair of particles come into contact, and the simulation is then continued. In the case of spheres, eventually the system becomes so congested that all particle moves are rejected, except for a handful of rattlers (i.e., incompletely arrested spheres) at the volume fraction of $\phi = 0.635$. While the method produces jammed states for spheres, the same cannot be said for rods. Here we found the rate at which the system was compressed, reduced rapidly as the density increased. Eventually, the compression became so slow that it was impossible to devise a clear criterion as to where the simulation should be stopped.

A method in the literature, which has been used for both spheres and short rods, is RSA [9,16,26,27]. The RSA in two dimensions has direct relevance to the adsorption of particles on a surface. While three-dimensional amorphous packings have been successfully obtained using RSA, any relation between these packings and an experimental granular packing is at best tenuous. A granular packing is obtained under conditions where the pressure compressing the system is totally dominant over any thermal fluctuations. Here the particles are no longer able to move due to the congestion created after being compressed to a minimal volume by a large pressure. In an RSA simulation, particles are placed in random positions and then they are never allowed to move; this is in contrast to a granular packing where highly collective rearrangements occur until congestion prohibits further movement. We observed that the final RSA packing volume fraction is never achieved on the computer due to the slow power law by which it is approached as a function of insertion attempts. Another disadvantage is that in the case of long rods, the RSA approach will no longer form an isotropic amorphous packing. Such a packing has a very low density due to the large excluded volume of a long thin rod. The RSA method will always be able to insert many more rods into an isotropic packing by finding the best possible way to align an insertion attempt. Such carefully inserted aligned extra particles do not occur in granular packings due to the extreme entanglement of the particles. The RSA process pays no heed to entanglement. A more realistic variation of the RSA method has been reported [29] where particles are only added to the surface, however only short rods have been studied.

It is clear that a new method of forming fibrous granular packings is necessary if the simulation work currently reported in the literature is to be significantly extended. The method we have developed is described next. In spirit, it is similar to an existing method that has been used for polydisperse spheres [30].

C. The mechanical contraction

In forming an amorphous packing, we are interested in what happens under conditions where the pressure on the system dominates over any thermal fluctuations. If a thermal system is to be quenched, the quench rate must be extremely high such that the particles are forced into permanent contact with each other on a time scale where the system cannot move towards a more thermodynamically favored phase as this would affect the final structure and density. Our technique for obtaining amorphous packings, referred to as the ''mechanical contraction,'' is based around the idea of density quenching a system, which undergoes no thermal fluctuations and it works as follows. A dilute equilibrium fluid of spherocylinders is prepared, in a cubic cell with periodic boundary conditions, using standard Monte Carlo techniques [31]. This is used as the initial configuration for the system, which is then squashed to obtain an amorphous packing. The volume of the cubic cell is reduced by a small amount ΔV and all of the particle positions are scaled by the factor

$$s = \left(1 - \frac{\Delta V}{V}\right)^{1/3}, \tag{2}$$

while their orientations are left undisturbed. Thus, all the particles are moved back inside the cell, however this results in some of the particles overlapping each other. The overlapping particles are then moved outside each other in an iterative manner (described below). The entire process is then repeated until the system becomes so congested that the overlapping particles can no longer be moved outside each other, if the system is contracted any further, and thus the final granular packing is obtained.

In order to describe how the overlapping particles are removed from each other, we first introduce some geometry and definitions. A spherocylinder may be represented by its axis of symmetry, a line of length L. Consider a pair of spherocylinders, both will possess a unique point on their axes of symmetry such that the distance between the two points is a minimum, the vector connecting these two points is labeled $\mathbf{k}$. If the magnitude k is less than the spherocylinder's diameter D, the two spherocylinders overlap. Once two spherocylinders are identified as overlapping the extent of the overlap is given by $\delta = D - k$. If there are C particles, which overlap with particle i, and particle i is moved with constant translational and rotational velocities then the speed at which particle i is changing its overlap with the contacting particle j may be quantified:

$$\frac{\partial \mathbf{k}_j}{\partial t} = k_j^{(1)} a_1 + k_j^{(2)} a_2 + k_j^{(3)} a_3 + l_j k_j^{(4)} a_4 + l_j k_j^{(5)} a_5. \tag{3}$$

Here generalized coordinates have been used, $n = 1$, 2, and 3 are the Cartesian coordinates of the system and $n = 4$ and 5 are two additional Cartesian coordinates that are perpendicular to each other and the axis of particle i. The variables a_n are the velocities of particle i, $n = 1$, 2, and 3 being the velocity of the particle's center of mass and $n = 4$ and 5 being the particle's rotational velocity. The orientation of particle i is given by the unit vector $\hat{\mathbf{p}}_i$ and the above mentioned rotational velocity is equal to $\partial \hat{\mathbf{p}}_i / dt$. The variable l_j is the distance from the ith particle's center of mass to the point of contact with particle j along the axis of particle i. In the case

where the contact is located on the opposite end of spherocylinder i to that pointed to by vector $\hat{\mathbf{p}}_i$, length l_j will take on a negative value. The variables $k_j^{(n)}$ are the components of vector $\mathbf{k}_j$ projected on to each of the five axes. We now write down the following equation, which is representative of the speed s, where a given particle is breaking contact with its C overlapping particles,

$$s=\sum_{j=0}^{C}\delta_j\frac{\partial \mathbf{k}_j}{\partial t}, \tag{4}$$

where the factor δ_j is included in order to bias the rate at which the particles break contact in favor of those which are overlapping the most. In order to proceed, we introduce a kinetic energy–type constraint on the velocity of particle i,

$$a_1^2+a_2^2+a_3^2+\xi a_4^2+\xi a_5^2=1, \tag{5}$$

where ξ is an arbitrary parameter which in the case of kinetic energy is simply related to the particle's moment of inertia. A Lagrange multiplier is then used in Eq. (4) with the constraint, Eq. (5), to obtain the direction in which to move particle i in order to reduce the degree of overlap with the C contacting particles at the maximum rate. The direction thus obtained in terms of the velocity vector with arbitrary speed is given for $n=1$, 2, and 3 as

$$a_n=\sum_{j=0}^{C}\delta_j\frac{k_j^{(n)}}{k_j} \tag{6}$$

and for $n=4$ and 5 as

$$a_n=\frac{1}{\xi}\sum_{j=0}^{C}\delta_j l_j\frac{k_j^{(n)}}{k_j}. \tag{7}$$

It should be pointed out that in the case of spheres the above procedure produces the same result as Eq. (6), there being only three dimensions for the direction a sphere moves. At this stage, it is possible to determine which direction each particle in the system is to be moved. However, the question remains as to how far each particle is to be moved. It was decided that each particle should move a very small distance, further than half the distance necessary to break the first contact. In the case where two particles are in contact with each other and only each other, this results in the pair being moved just far enough to break contact. The extra distance was specified such that slightly larger spherocylinders would break contact ($\approx$1.0001 times bigger in diameter), this helped alleviate problems with more contacts being made as the particles are moved and with a finite machine precision. The direction and distance each particle needs to be moved is calculated and then they are all moved. This is then repeated a large number of times until there are no more overlapping pairs of particles. If an arbitrarily chosen cutoff number of iterations is reached without all the particles breaking contact, it will be deemed that the system had reached its highest packing density. Given that the iteration cutoff number is large enough, the final result is not sensitive to its choice.

While this technique produces a good representation of granular packing for spheres and short rods, this is not the case for long rods. In the later case, the technique does not sufficiently sample rearrangements, which involve particles sliding along their own axis of symmetry. This is overcome by squashing the system as much as possible using the mechanical contraction technique followed by a series of Monte Carlo moves where all move attempts are in a direction parallel to the particles own axis of symmetry. The system is then subject to the mechanical contraction technique again and the process is repeated until the system can no longer be reduced in volume. In the case of short spherocylinders (aspect ratios less than 4.0), this makes absolutely no difference. In the case of very long spherocylinders (aspect ratios above 100), it can allow further reduction of the system's volume by a factor greater than 2.0. Eventually, a well defined and reproducible maximum density is obtained.

A version of the Verlet neighbor list [32], modified for spherocylinders, is used. The distance k between each pair of rods is used to construct the list and the distance each end of a rod moves is then monitored in order to determine when the list needs to be updated. This is done when either end of a rod moves further than $(r_{\mathrm{cut}}-D)/2$, where r_{cut} is the cutoff radius used to form the list.

D. Simulation details

The final configurations were analyzed using a generalization of the radial distribution function to handle spherocylinders. Here, the distance k (see Sec. II C) between the two spherocylinders was used in place of the distance between the centers of a pair of spherical particles. The number of particles in a structureless system, which would be expected to be found tangential to a spherocylinderical shell of radius k, thickness dk, and a length L equal to that of the particles under consideration is used to normalize the distribution function. This may easily be calculated by differentiating Eq. (8) with respect to the spherocylinderical shell's radius and then multiplying by the shell thickness dk.

A range of aspect ratios was investigated from spheres to long spherocylinders $0\leqslant\alpha\leqslant 160.0$. The number of particles used in the simulation depended heavily on the aspect ratio. This is because spherocylinders require a simulation box that is at least twice their length to satisfy the minimum image condition. In the case of long rods, the packed volume fraction asymptotes to $\phi\sim 1/\alpha$ and the volume of each rod (with constant diameter) asymptotes to $v_p\sim\alpha$, so that we can expect the required number of particles to be proportional to the aspect ratio $N\sim\alpha$. In the case of $\alpha=160.0$, the necessary number of particles was $N=42$ and 592.

Dilute isotropic fluids, in thermal equilibrium, were first prepared using a standard canonical Monte Carlo algorithm. The system was then subject to the mechanical contraction with a maximum of 10^3 iteration attempts and $\Delta V/V=10^{-3}$. Eventually, a density was reached where all the rods or spheres could no longer reach a state, with no overlapping pairs, within the specified number of iteration attempts. The value of ΔV was then scaled down, typically by a factor of 0.1 but sometimes a value closer to unity, depending on what

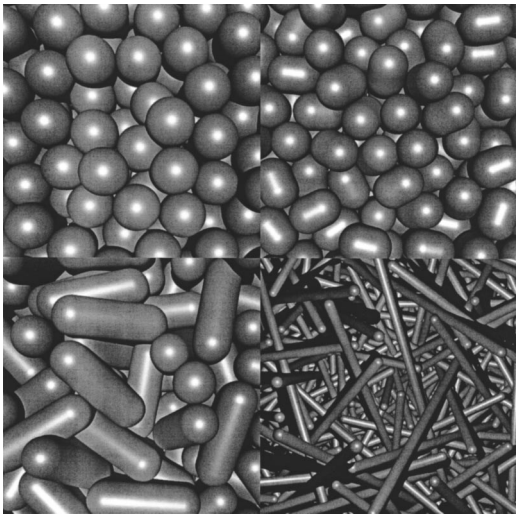

FIG. 1. Images (ray tracings) of tightly packed isotropic spherocylinders for several aspect ratios α. Aspect ratios of (clockwise from top left) $\alpha=0$ (spheres), $\alpha=0.4$, $\alpha=40.0$, and $\alpha=2.0$. For $\alpha=0.4$, the highest packing density $\phi=0.70$ is achieved (see Fig. 2). The packing for $\alpha=2.0$ is already to the right of the density maximum, and has a density $\phi=0.616$, which is close to that of the random sphere packings.

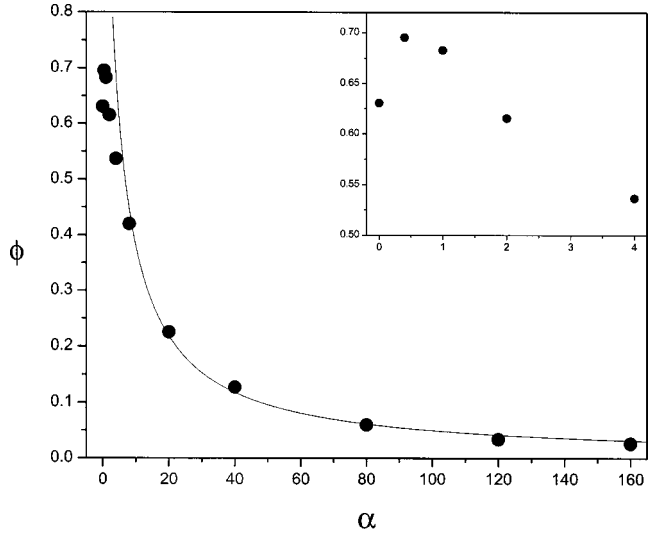

FIG. 2. Final volume fractions ϕ for the amorphous packings as a function of aspect ratio α. The solid line is a theoretical fit from the random contact equation $\phi\alpha=5.1$ [see Eq. (1)]. The inset shows a magnified view of the same graph at low aspect ratio.

seemed to reach the final result most expediently. Eventually, ΔV became so small that it was less than the least significant bit in the machine storage of the value for V, at this stage the system was deemed to have reached its final volume. In the case of long rods (aspect ratio $L/D \geqslant 8$), the system was subject to the Monte Carlo moves along the rods axis as described above.

III. RESULTS AND DISCUSSIONS

When applied to spheres, the mechanical contraction method forms a randomly packed configuration with a volume fraction of $\phi=0.631$ and a radial distribution function, which may be seen in Fig. 3. These results are consistent with previous studies on random packings of hard spheres by both colloidal experiments [33] and simulation [22].

A. Aspect ratio dependence

The results obtained for spherocylinders depended strongly on the aspect ratio α. Images (formed by ray tracing) of the random packings for several aspect ratios may be seen in Fig. 1 and volume fractions, of the random packings, obtained as a function of aspect ratio are shown in Fig. 2. It can be clearly seen that the very short rods pack to higher volume fractions than the spheres, with a maximum (from the aspect ratios studied) of $\phi=0.695$ for $\alpha=0.4$. A qualitatively similar trend has been found for the RSA of spheroids [16] and Monte Carlo simulations of the pouring of elliptical particles in two dimensions [17,18] and ellipsoids in three dimensions [19] suggesting that small deviations in the shape of identical spherical particles allow a more efficient amorphous packing. It is well known that an amorphous polydisperse system of spheres packs more efficiently than an equivalent monodisperse system [30]. To understand this, consider a system of amorphously packed spheres. We can expect the interstices between the spheres to all be small enough such that no additional spheres can be placed in them. If the system is made more polydisperse, the smaller spheres may be placed where the larger ones previously could not. So the size variation allows for more efficient amorphous packing. Perturbing the particle shape from spherical has a similar affect to size variation: a short spherocylinder that may not fit in an interstice when orientated in a given direction may fit when the orientation is changed. On the contrary, the orientationally averaged excluded volume [34,35] of the spherocylinder will change with the aspect ratio and hence also affect the efficiency of the packing:

$$E=\frac{6\alpha^2+24\alpha+16}{2+3\alpha}. \tag{8}$$

Here, $E=v_{\mathrm{ex}}/v_p$ is the excluded volume divided by the particle's volume and α is the aspect ratio. Now Eq. (8) has a very weak dependence on the aspect ratio α when it is small, so the size variation effect dominates and the short spherocylinders pack more efficiently than do the spheres. For spheres, the aspect ratio is $\alpha=0$ and the reduced excluded volume is $E=8$, and for short spherocylinders with aspect ratio $\alpha=0.4$, the excluded volume will be such that $E=8.3$. For large aspect ratios, E increases strongly with aspect ratio α and the effect of the excluded volume completely dominates. At large aspect ratios, the volume fraction decreases in a manner that is inversely proportional to the aspect ratio. This dependence is also found experimentally [5,11] and predicted by the random contact scaling for long rods, Eq. (1) [5]. This is a direct consequence of the packing being determined by the excluded volume per particle, while the average number of contacts per particle remain constant [5]. Fitting the simulation data to Eq. (1) provides the aver-

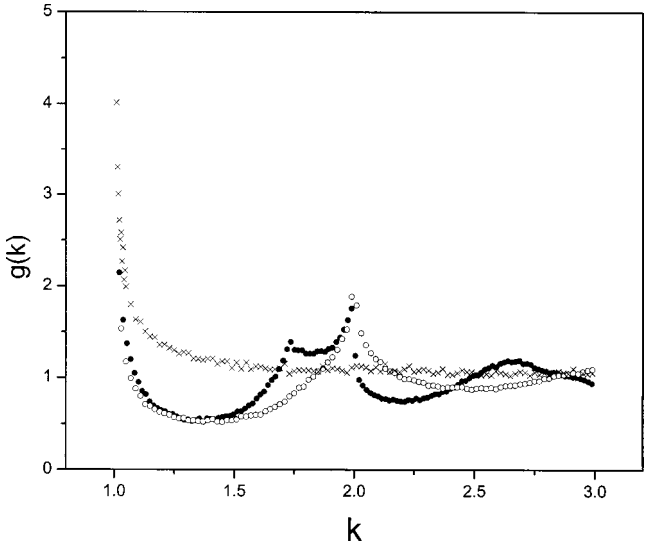

FIG. 3. Generalizations of the radial distribution function for spheres (closed circles), spherocylinders of aspect ratios $\alpha=2.0$ (open circles) and 80.0 (crosses). k is the shortest distance between the two rods axes of symmetry in units of the rods diameter.

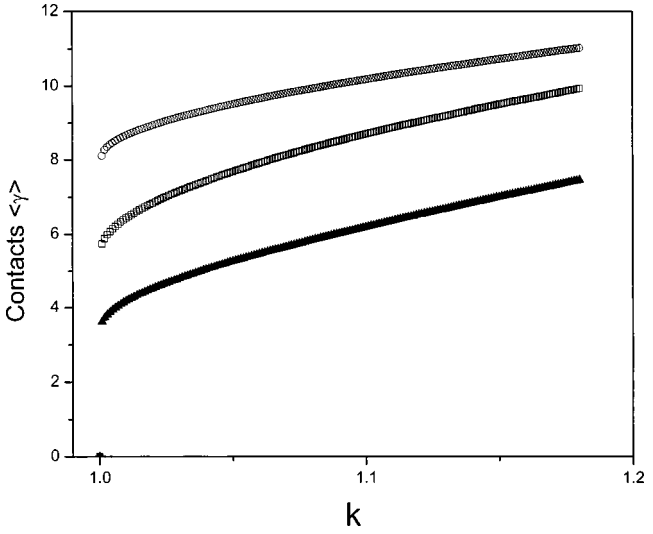

FIG. 4. Number of contacts, as a function of minimum distance between rods symmetry axis k, for spheres (squares) and rods with aspect ratios $\alpha=2.0$ (circles) and 80.0 (triangles).

age contact number $\langle\gamma\rangle=10.2$, which agrees well the value of $\langle\gamma\rangle=10.8\pm0.4$ obtained for experimental rod packings [5].

We note here the use in the literature [7] of an empirical correlation to predict trends in packing densities of nonspherical particles from the sphericity parameter,

$$\psi=4.87\frac{v_p^{2/3}}{s} \tag{9}$$

which characterizes the shape of a particle with volume v_p and surface area s. For a sphere $\psi=1$, and for thin rods,

$$\psi=1.32\alpha^{-1/3}, \quad \alpha\gg1. \tag{10}$$

It is clear that ψ predicts the wrong scaling for thin-rod packing densities.

B. Radial distribution and contact numbers

In a thermal system of hard particles, on an average, there will be no pairs of particles in contact with each other. In a granular packing, the pressure totally dominates over the thermal fluctuations. This causes pairs of particles to remain in constant contact with each other. Calculating the exact number of contacts from the final simulation configuration is not a trivial task. Perhaps the most straightforward approach is to search for the number of particles within a certain distance of the central particle. To further investigate the validity of this, a generalization of the radial distribution function (commonly used with spherical particles) for spherocylinders of aspect ratios $\alpha=2.0$ and 80.0 is presented in Fig. 3. For the shorter spherocylinders, $\alpha=2.0$, there is a sharp peak at the contact distance followed by a depletion region. There is also a second much smaller peak due to a pair of particles having an additional particle between them, which is analogous to the second peak in the radial distribution function for spheres. For the longer spherocylinders, $\alpha=80.0$, the sharp peak at contact is not followed by a depletion region. Rather, the function monotonically decays to the nonstructural value of unity. That the distribution function decays to some value approaching the nonstructural value at a distance k much less than the rods length L is indicative of the system being relatively free from local structural alignment. This seems to be a more sensitive way of identifying a small degree of local alignment in long rods than the nematic order parameter. What is clear from Fig. 3 is that defining any particles, which are within a certain distance from each other, to be in contact will be a definition that is affected by the aspect ratio. However, from spheres to long rods there is a very sharp peak in the radial distribution function near contact. The number of contacts as a function of separation distance is shown in Fig. 4 for rods of aspect ratio $\alpha=2.0$ and 80.0. While the definition of any particles closer than a certain distance has problems, it may be used as a meaningful working definition, especially for short rods and spheres.

C. Random contact equation

The numbers of contacts per particle, determined from plots as in Fig. 4, as a function of the aspect ratio are shown in Fig. 5. along with the volume fractions obtained from the random contact equation and those obtained directly from the simulations. In the case of randomly positioned, noninteracting long rods, the common volume of any overlapping rods will be insignificantly small as compared to the rod's excluded volume in an interacting system. Isotropic systems of long rods therefore have very little structure (see Fig. 3.). Such weak correlations support the proposition [5] that the overlapping rods of a noninteracting system are equivalent to the contacting rods of a corresponding random thin-rod packing. This gives the random contact equation, which states that

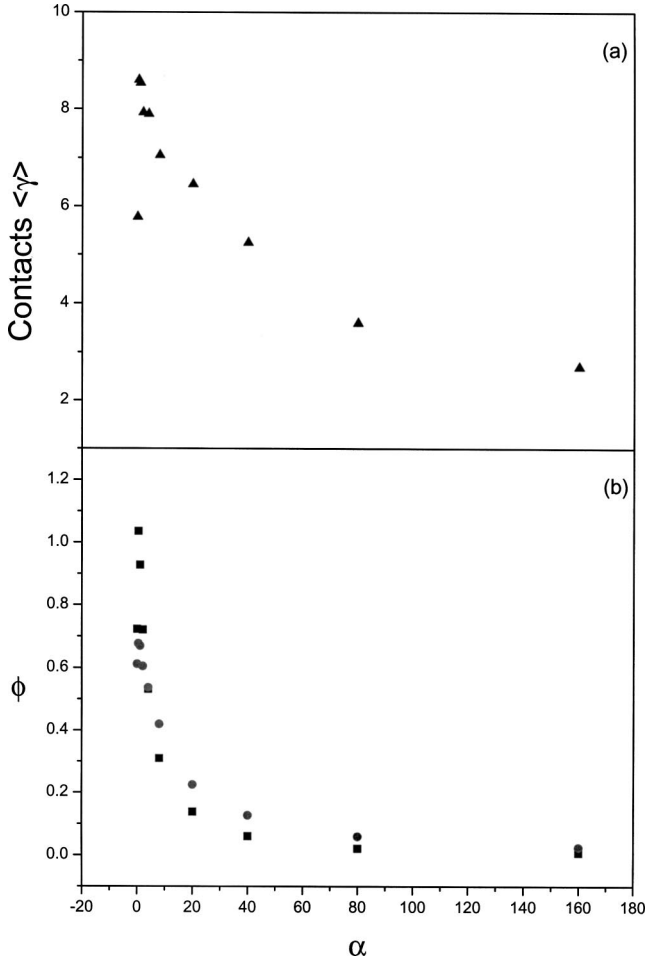

FIG. 5. In Fig. 5(a), the number of contacts as a function of aspect ratio (triangles) are shown. In Fig. 5(b), volume fractions ϕ obtained directly from the simulations are compared to those calculated from the average number of contacts using the random contact equation. The simulation data as presented in Fig. 1 (squares) and the random contact volume fractions (circles) are shown as a function of aspect ratio.

$$\phi E = \langle \gamma \rangle = \frac{1}{N} \sum_{i}^{N} \gamma_i , \tag{11}$$

where γ_i is the number of particles in contact with the ith particle. In other words, for a given particle shape (fixed E), the density is determined by the average of γ. This average coordination number, in turn, may be fixed by the requirement that a rod is immobilized (caged) by its neighbors. The average minimal number (the caging number) of neighbors to achieve such caging is $\langle \gamma \rangle = 4.79$ for three-dimensional spheres [36]. For spherocylinders, caging numbers have not been calculated yet, though it has been shown that the lower bound for thin rods is, $\langle \gamma \rangle \geqslant 5$ [37], with a corresponding packing density bound of $\phi\alpha > 2.5$, which incidentally is consistent with experiments and our simulations. It has been argued [5] that whatever the precise value for γ, it will be invariant to the aspect ration for $\alpha \gg 1$. The argument is that if a certain number of neighbors cage a thin rod, the caging situation will not change as the rod is pulled out to higher

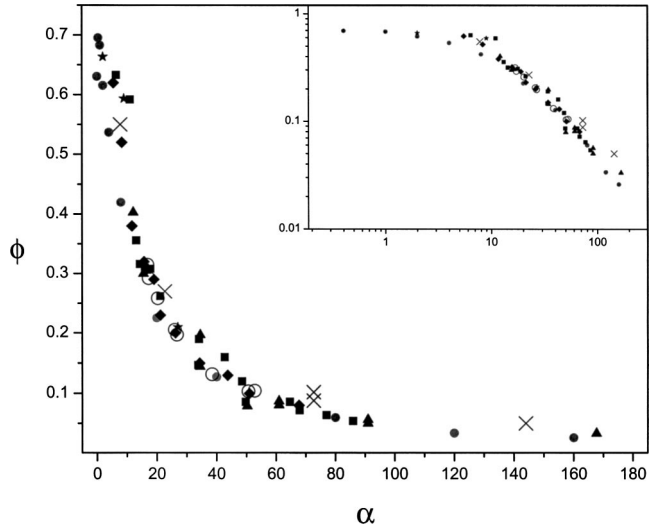

FIG. 6. Comparison between simulation and experimental packing densities compiled from Refs. [1,5,10–14,45]. The inset shows a logarithmic plot of the same data.

aspect ratios. Combining this idea with Eqs. (8) and (11) predicts that the volume fraction will be inversely proportional to the aspect ratio $\phi \sim \alpha$ for very long rods. This can easily be seen by replacing the excluded volume in Eq. (11) with the infinitely long rod expression (as used by Onsager [34,35]), which gives Eq. (1). Figure 5 depicts a direct test of Eq. (11) with plots of both $\langle \gamma \rangle$ and ϕ being obtained directly from the simulation and a second volume fraction ϕ_{rc} obtained from Eq. (11) using the number of contacts $\langle \gamma \rangle$ from the simulation. Not only does this explain the behavior of the long rods, but it also provides a qualitative insight into the behavior of the very short rods (i.e., an alternative explanation of the increased volume fraction for very short spherocylinders). For very short spherocylinders, the excluded volume depends only weakly on the aspect ratio as opposed to the number of contacts necessary to cage the spherocylinder. As the aspect ratio increases, more contacts are required to cage the particle requiring a higher volume fraction. At still higher aspect ratios, the required number of contacts plateaus however the excluded volume increases significantly and drives the volume fraction back down.

Quantitatively, the contact number for long rods obtained directly from the simulations $\langle \gamma \rangle = 3$ is significantly different from that obtained from Eq. (11) $\langle \gamma \rangle = 10$. This is due to the rods having an effectively larger diameter due to the structure near contact Fig. 3.

D. Comparison to experiments

Our simulation results for the random packing densities agree fairly well with the available experimental densities, compiled in Fig. 6. Most experiments relate to granular rods or fibers in the centimeter size range from a variety of materials such as wood [1], metal wire [5], and raw spaghetti [12]. Also packings of anisotropic colloids are included [5]. The scatter in the experimental densities may be due to factors such as wall effects, friction between particles, occasional local nematic ordering, and particle flexibility.

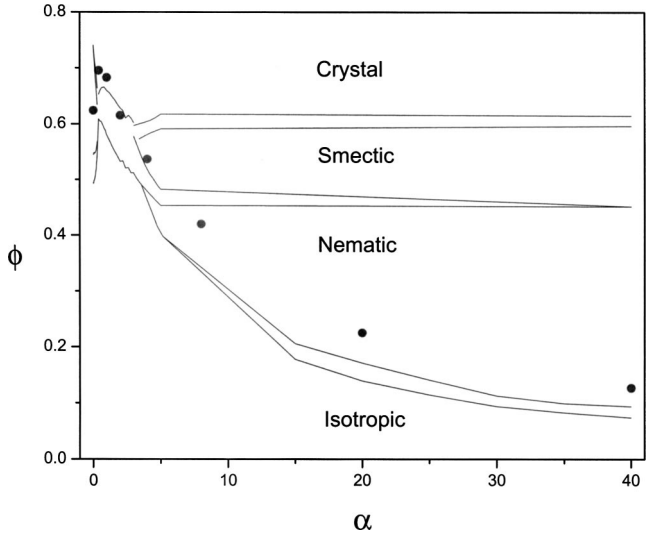

FIG. 7. Simulation volume fractions as presented in Fig. 1 (solid circles) shown with the known equilibrium phase diagram [39] for spherocylinders. The solid lines show the phase boundaries.

Nevertheless, the data clearly confirm that our simulation models random packings very well. The data also exhibit the asymptotic scaling of Eq. (1), with a value $c=5.4\pm0.2$ which agrees with the value $c=5.1$ from the simulation. The experimental data are less clear with respect to the packing density on approach of the sphere shape. The Bernal sphere packing density $\phi=0.64$ is confirmed, but the maximum near $\alpha=0.4$ has not been identified, simply because packing data relate to $\alpha>1$. It should be noted that even a small polydispersity in shape affects the density near $\alpha=1$ considerably: quite monodisperse particles will be needed to observe the density maximum in Fig. 2. For granular objects, this monodispersity is feasible; as of yet we do not have relevant data on cylinders or prolates. However, for oblate particles, we indeed observe a density maximum [38].

A comparison between the known equilibrium equation of state for hard spherocylinders [39] and the granular packing volume fractions may be seen in Fig. 7. It can readily be seen that it is possible to compress an isotropic system of spherocylinders to a density where the nematic phase is the equilibrium state. For rods having an aspect ratio of $L/D\approx4.0$, the granular packing density is such that the equilibrium phase is smectic. However, for larger aspect ratios, it is not possible to compress a system to a density high enough so that the smectic phase is the equilibrium one. So if, for example, an experimental sample of colloidal hard rods is to be frozen into the smectic phase, it will have to do so via the nematic phase, not straight from the isotropic phase. Amorphous systems of very short rods can be quenched to a density where the crystalline state is the equilibrium one. For aspect ratios around $\alpha\approx0.8$, the granular packings are so dense that the orientationally ordered solid phase is the equilibrium state.

E. Glass transition

Not only does size variation allow for more efficient amorphous packings of spheres, it also effects the glass transition [40]. It is to be expected that a possible glass transition volume fraction for hard spherocylinders, as a function of aspect ratio α, will have a strong correlation to the amorphous packing volume fractions. This, incidentally, says nothing about whether a thermally long-lived glassy phase can indeed be formed. In the case of identical spheres, there is no stable glassy phase, however, this may be remedied with the introduction of a small amount of polydispersity [41]. It seems quite likely that there will be a long-lived dense metastable phase for long rods due to the extreme tangling between them. Indeed, colloidal rods form long-lived isotropic structures after sedimentation [42]. In the case of shorter rods, things could depend very critically on the aspect ratio. Here the amorphous phase may become stable due to the competition between competing equilibrium phases as there are many phase boundaries around the packings of short rods.

Upon undercooling, a liquid falls out of equilibrium (due to nonergodicity) across a narrow transformation range [43], thus sensible operational definitions of where the glass transition occurs show reasonable compatibility. This is the case even for measures based on conflicting fundamental principles. For molecular glasses, the translational diffusion decouples from the viscosity, however the rotational diffusion does not [43]. According to the tube model of Doi and Edwards [44], the rotational diffusion will slow down inverse squarely proportional to the volume fraction $D_L^r\propto\phi^{-2}$, which is not compatible with the expected viscous behavior of a glassy liquid. The details and even the existence of a glassy phase formed from long rods remains an open question.

IV. CONCLUSIONS

The mechanical contraction method for obtaining granular packings has been introduced. This has resulted in amorphous granular packings of spheres, which are consistent with previously used methods. Further, the method is able to handle spherocylinders out to very long aspect ratios. It should be possible to study other shapes such as ellipsoids and disks using the methods that have been introduced in this paper. The results for the spherocylinders reproduce existing experimental results for all available aspect ratios. The volume fractions of the long spherocylinders confirm the prediction that the random packing density of thin rods is inversely proportional to the aspect ratio. In addition, the expectation is confirmed that spatial correlations gradually vanish with increasing aspect ratio. The random sphere packing density turns out to be a local minimum: the highest density occurs at an aspect ratio of $\alpha\approx0.4$. The practical implication is that a small deviation in shape from spherical may increase the random packing density significantly without crystallization. If it is assumed that spherocylinders form a stable thermal glassy phase, it can be expected to occur at very low densities for large aspect ratios. Finally, our simulations clearly show that particles with a given aspect ratio have a unique random packing density: The Bernal sphere packing can be generalized to spherocylinders of arbitrary

aspect ratio with one and the same simulation method. This indicates that these packings all follow the same geometrical principle(s). The (at least qualitative) applicability of Eq. (11) suggests that the random packing density is, for all aspect ratios, the outcome of a competition between coordination numbers (determined by local caging effects) and excluded volumes.

ACKNOWLEDGMENTS

We are grateful to Gijsje Koenderink and Willem Kegel for fruitful discussions. This work was a part of the research program of the Foundation for Fundamental Research on Matter (FOM) with financial support from The Netherlands Organization for Scientific Research (NWO).

[1] J. V. Milewski, in *Handbook of Fillers and Reinforcements for Plastics*, edited by H. S. Katz and J. V. Milewski (Van Nostrand Reinhold, New York, 1978).
[2] C. T. J. Dodson, Tappi J. **79**, 211 (1996).
[3] L. Spielman and S. L. Goren, Environ. Sci. Technol. **2**, 279 (1968).
[4] G. W. Jackson and D. F. James, Can. J. Chem. Eng. **64**, 364 (1986).
[5] A. P. Philipse, Langmuir **12**, 1127 (1996); **12**, 5971 (1996) (Correction).
[6] D. Bideau and A. Hansen, *Disorder and Granular Media* (North-Holland, Amsterdam, 1993).
[7] D. J. Cumberland and R. J. Crawford, *The Packing of Particles* (Elsevier, Amsterdam, 1987).
[8] T. Aste and D. Weaire, *The Pursuit of Perfect Packing* (Institute of Physics, Bristol, 2000).
[9] K. E. Evans and M. D. Ferrar, J. Phys. D **22**, 354 (1989).
[10] K. E. Evans and A. G. Gibson, Compos. Sci. Technol. **25**, 149 (1986).
[11] M. Nardin, E. Papirer, and J. Schultz, Powder Technol. **44**, 131 (1985).
[12] M. Novellani, R. Santini, and L. Tadrist, Eur. Phys. J. B **13**, 571 (2000).
[13] J. G. Parkhouse and A. Kelly, Proc. R. Soc. London, Ser. A **451**, 737 (1995).
[14] O. Rahli, L. Tadrist, and R. Blanc, C. R. Acad. Sci., Ser. IIb: Mec., Phys., Chim., Astron. **327**, 725 (1999).
[15] D. M. Bigg, in *Metal Filled Polymers*, edited by S. K. Bhattacharya (Dekker, New York, 1986).
[16] J. D. Sherwood, J. Phys. A **30**, 839 (1997).
[17] B. J. Buchalter and R. M. Bradley, J. Phys. A **25**, 1219 (1992).
[18] B. J. Buchalter and R. M. Bradley, Phys. Rev. A **46**, 3046 (1992).
[19] B. J. Buchalter and R. M. Bradley, Europhys. Lett. **26**, 159 (1994).
[20] W. G. Hoover and F. H. Ree, J. Chem. Phys. **49**, 3609 (1968).
[21] P. A. Buining and H. N. W. Lekkerkerker, J. Phys. Chem. **97**, 11510 (1993).
[22] B. D. Lubachevesky, F. H. Stillinger, and E. N. Pinson, J. Stat. Phys. **64**, 501 (1991).
[23] E. L. Hinrichsen, J. Feder, and T. Jøssang, Phys. Rev. A **41**, 4199 (1990).
[24] S. Torquato, T. M. Truskett, and P. G. Debenedetti, Phys. Rev. Lett. **84**, 2064 (2000).
[25] L. E. Silbert *et al.*, Phys. Rev. E **65**, 031304 (2002).
[26] E. L. Hinrichsen, J. Feder, and T. Jøssang, J. Stat. Phys. **44**, 793 (1986).
[27] D. W. Cooper, Phys. Rev. A **38**, 522 (1988).
[28] B. D. Lubachevesky and F. H. Stillinger, J. Stat. Phys. **60**, 561 (1990).
[29] D. Coelho, J. F. Thovert, and P. M. Adler, Phys. Rev. E **55**, 1959 (1997).
[30] D. He, N. H. Ekere, and L. Cai, Phys. Rev. E **60**, 7098 (1999).
[31] D. Frenkel and B. Smit, *Understanding Molecular Simulation From Algorithms to Applications* (Academic Press, San Diego, 1996).
[32] M. P. Allen and D. J. Tildesley, *Computer Simulation of Liquids* (Clarendon Press, Oxford, 1989).
[33] A. van Blaaderen and P. Wiltzius, Science **270**, 1177 (1995).
[34] L. Onsager, Ann. N.Y. Acad. Sci. **51**, 627 (1949).
[35] G. J. Vroege and H. N. W. Lekkerkerker, Rep. Prog. Phys. **55**, 1241 (1992).
[36] E. A. J. F. Peters *et al.*, Phys. Rev. E **63**, 021404 (2001).
[37] A. P. Philipse and A. Verberkmoes, Physica A **235**, 186 (1997).
[38] A. P. Philipse and G. Koenderink (unpublished).
[39] P. Bolhuis and D. Frenkel, J. Chem. Phys. **106**, 666 (1997).
[40] S. R. Williams and W. van Megen, Phys. Rev. E **64**, 041502 (2001).
[41] S. R. Williams, I. K. Snook, and W. van Megen, Phys. Rev. E **64**, 021506 (2001).
[42] A. P. Philipse, A. M. Nechifor, and C. Patmamanoharan, Langmuir **10**, 4451 (1994).
[43] P. G. Debenedetti and F. H. Stillinger, Nature (London) **410**, 259 (2001).
[44] M. Doi and S. F. Edwards, *The Theory of Polymer Dynamics* (Oxford University Press, Oxford, 1986).
[45] O. Rahli, Ph.D. thesis, Université de Provence, 1997 (unpublished).